Role of energy partitioning on electron-hole recombination, trapping, and detection in silicon detectors

Yanwen Zhang[1,2,*] and William J. Weber[2,1]
[1]*Materials Science & Technology Division, Oak Ridge National Laboratory, Oak Ridge, Tennessee 37831, USA*
[2]*Department of Materials Science & Engineering, University of Tennessee, Knoxville, Tennessee 37996, USA*
(Received 30 May 2010; published 5 August 2010)

The dynamics of electron-hole pair creation and transport in a semiconductor control the fundamental signal response for radiation detection. Extensive studies on silicon detectors have led to contradictory interpretations on the origins of the pulse height defect (PHD) and nonlinear response. In this study, recombination and trapping behaviors of a controlled number of electron-hole pairs produced within different volumes along the ion path are investigated, and the pulse height generated is analyzed in terms of energy partitioning. The results clearly demonstrate that a high recombination rate is not observed for heavy ions; moreover, significant trapping associated with the atomic defects produced by individual ions is responsible for the nonlinear response at low energies and PHD at high energies.

DOI: 10.1103/PhysRevB.82.075202 PACS number(s): 72.20.Jv, 07.77.Ka, 29.40.Wk

I. INTRODUCTION

Knowledge on electron-hole (e-h) pairs created by a primary charged particle at a given energy and the nonlinear response of the material is fundamental to advanced detector design, device performance in high radiation fields, detector applications in high-energy physics, ion-beam analysis, medical applications, national security, as well as for characterizing single event upsets in electronics for space and missile applications, development of advanced sensors, and diagnostics for use in extreme environments. Under ion irradiation, energy is lost to both electrons and atoms in materials. Kinetic-energy transfer to target electrons, electronic energy deposition (dE/dx_{ele}), produces e-h pairs. Energy transfer to target atoms, nuclear energy deposition (dE/dx_{nucl}), can result in recoil and displacement of atoms from their original sites, thereby forming atomic-scale defects and producing more e-h pairs if the recoils are sufficiently energetic. In a semiconductor, e-h pairs are the fundamental information carriers, and their motion in an electric field generates the basic electrical pulse.

The measured number of e-h pairs created by a primary charged particle and the deviation from the ratio between the number and particle energy (nonlinear response or differential pulse height) at different energies are critical properties for detector applications. There have been intensive studies on the mechanisms of e-h pair recombination, diffusion, trapping, and detection in silicon detectors, and contradictory interpretations started in 1960s and continue to this day.[1–12] The pulse height defect (PHD), a circumvent problem for detecting heavy ions, is normally defined as the difference between the true energy of the heavy ion and its apparent energy, as determined from an energy calibration of the detector using protons or alpha particles.[1] Three origins to the observed PHD and nonlinear response are generally accepted: (1) energy loss of the ion in the contact layer of the detector, (2) energy loss not contributed to e-h pair productions, such as the energy transferred to atoms, and (3) the high rate of e-h recombination in the dense plasma created along the ion track by heavy ions.[3–11] In the present study, the response of a silicon detector to single-ion excitation is studied for different ions over a continuous energy region to evaluate the different origins to the PHD and nonlinearity. The relative pulse height, the height difference resulting from a small amount of energy deposition, is analyzed as a function of the corresponding electronic stopping power, where a constant energy loss; i.e., constant plasma density, can be assumed over a small depth. Such an approach has major advantages over earlier analyses in which the pulse height has been described as a function of total ion energy, where the plasma density varies as the ion slows down in Si. After corrections for origins (1) and (2), the current results clearly demonstrate that the e-h recombination rate is not higher for heavy ions. Moreover, significant trapping of the e-h pairs is explicitly observed with increasing numbers of atomic defects created through nuclear collisions by individual ions, and such trapping leads to non-negligible PHD with increasing ion mass.

II. EXPERIMENTAL DETAILS

The experimental setup for the e-h pair measurement consists of a time of flight (TOF) telescope[13,14] followed by a silicon detector. The two carbon-foil timing detectors, separated by a flight length (L_{TOF}), are used to determine the energy of individual particles before impinging on the silicon detector. When an energetic particle passes though the carbon foil ($\sim$4–10 μg cm^{-2} depending on the ions of interests), electrons are emitted and collected by microchannel plates (MCPs). If the signal produced from the MCPs exceeds the constant fraction timing discriminator threshold, the particle is detected by the timing detector. The silicon detector is placed after the second time detector with a collimator (10 mm in diameter) in front of it.[13,14] Energetic particles of H^+, He^+, Be^+, Si^+, and S^+ produced from a tandem accelerator were forward scattered into the TOF telescope by a thick Au target to produce particles with a continuous distribution of energies, from a few tens of keV to a few MeV per atomic mass unit (amu). To avoid confusion, silicon ions will be noted as Si^+, and silicon material will be

 ©2010 The American Physical Society

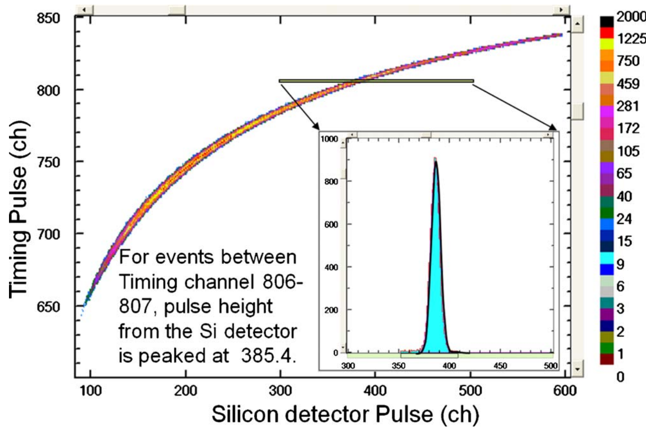

FIG. 1. (Color online) TOF pulse height versus pulse height from the silicon detector to proton ions. The inset is an example of the data analysis. For proton ions with energy between TOF channel of 806 to 807, the corresponding pulse height is peaked at channel 385.4.

noted as silicon in the current paper. Only a fraction of the scattered ions in a small solid angle pass through the two timing detectors and hit the silicon detector. The rate of charged particles hitting the silicon detector is controlled to be lower than a few events per millisecond; therefore, timing between each event is much longer than the time needed for each ion-silicon interaction event and signal processing. The pulse height in the silicon detector due to ion energy deposition is simultaneously recorded with the exclusive time of flight information of the ion, and the energy of each ion impinging on the silicon detector is, therefore, determined using the corresponding TOF information on a particle by particle basis. For each particle, the energy is determined as

$$E(\text{keV}) = \frac{1}{2}Mass\left(\frac{L_{\text{TOF}}}{\text{TOF(ns)}}\right)^2 - \Delta E_{\text{foil}}, \quad (1)$$

where *Mass* is the particle mass, TOF(ns), is the time for the ion to pass through the flight length (L_{TOF}), and ΔE_{foil} is the correction for the slight energy loss in traversing the carbon foil of the second timing detector that is the product of the electronic stopping power and the corresponding carbon-foil thickness. The time calibration[15] of the TOF telescope, a linear relationship between the TOF(ch) and TOF(ns), was obtained using both the signals of the ions that are scattered from the surface of the Au target and a timing calibrator (ORTEC module 462 from ORTEC, Oak Ridge, TN), with the two independent results validating each other to achieve a reliable time calibration. Depending on the actual thickness of the carbon foil used in each measurement, the typical time calibration is ~0.042 ns per channel.

A two-dimensional plot of TOF signals versus the silicon "detector response" to energetic protons is shown in Fig. 1, which is representative for other ions. Each data point represents one incident proton. The plot illustrates the continuous nature of the ion energies. The output signal from the first timing detector is delayed and fed together with the signal from the second timing detector to a time-to-amplitude converter in an inverse start-stop mode in order to minimize the dead time. Only the events that are registered by both time detectors and the silicon detector are considered. Fast response of the TOF telescope with a rise time of 210 ps allows quantitative and efficient evaluation of silicon response to ion energy deposition. In 10 min, more than one million H^+ ions were recorded by both the silicon detector and TOF telescope in coincidence mode, which demonstrates the measurement efficiency. The exclusive relation between TOF [ion energy, E(keV)] and the silicon detector response [pulse height, E(ch)] is illustrated by the inset, where the smooth solid line is a Gaussian fit to the data. The results in Fig. 1 indicate that H^+ ions with timing signals at channel of 806.5 produce pulses detected by the silicon detector centered at channel of 385.4 with a full width at half maximum (FWHM) of ~10.6. There are a number of contributions that lead to signal variance and contribute to the overall FWHM, and the detailed analysis has been described elsewhere.[16]

Because it is more stable and less subject to ambient conditions, an ion-implanted detector is used in the current study rather than a surface barrier detector. The silicon detector is an ion-implanted-silicon charged-particle detector from ORTEC (Oak Ridge, TN, USA), with an entrance contact consisting of an extremely thin layer (~520 Å) that was fabricated by boron implantation. The basic detector configuration is based on a fully depleted reverse-biased diode structure. Incident charged particles transfer their energy through collisions to target nuclei that may produce atomic defects and energetic secondary recoil atoms, and to electrons that produce excitation/ionization of atoms along a plasma column. Electron-hole pairs created by the passage of the incident ion and recoil atoms are separated by a strong electric field produced under an external bias. Electrons drift toward the anode, holes to the cathode, producing a current pulse on the electrode, which is collected by a charge-sensitive preamplifier.

III. RESULT AND DISCUSSIONS

The energy loss of the ion in the contact layer of the detector ($\Delta E_{\text{contact}}$), origin (1), can be corrected by the product of the electronic stopping power of the ion at the energy entering the detector and the thickness of the entrance layer (~520 Å). The impact of origin (1) to the nonlinear response of silicon is illustrated in Fig. 2 for ^{4}He, ^{9}Be, and ^{32}S ions. The dashed lines indicate the ideal response of silicon with a linear response and without PHD. Response for ^{1}H and ^{28}Si ions (not shown) is similar to that for the ^{4}He and ^{32}S ions, respectively. The nonlinear response for "Detector response" (the lower curve) is determined as the measured pulse height normalized to its energy [$E(\text{ch})/E_{\text{ion}}$] for each ion event, the response for "Origin (1) corrected" (the middle curve) is the measured pulse height normalized to the ion energy deposited in the detector active volume ($E_{\text{ion}} - \Delta E_{\text{contact}}$). The contribution of origin (1) to the nonlinear response, as shown by the difference between the middle and lower curves, is more significant at lower energies. Even after correction for energy loss in the contact layer, a nonlinear response (the curvature) still exists for all the ions, including He^+ ions. Furthermore, a clear PHD for the silicon

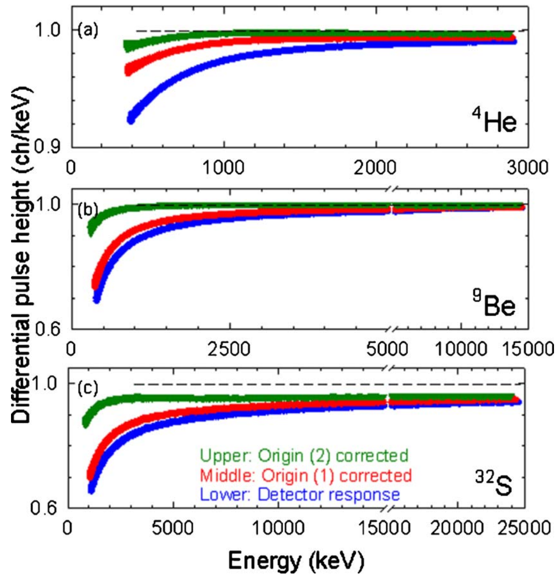

FIG. 2. (Color online) Differential pulse height to ^{4}He, ^{9}Be, and ^{32}S ions as a function of particle energy before (lower curve) and after (middle curve) the correction of the energy loss of the ion in the contact layer. The upper curve is the response after the correction of nuclear energy. Ideal response of the silicon detector with a linear response and without PHD is indicated by the horizontal dashed lines with the unity value determined by H^+ ions.

detector is evident as shown by the difference between the middle curve and the corresponding dashed line at high energies, which becomes increasingly significant with increasing ion mass, such as S^+ ions.

The nonlinear response of silicon after correction for origin (1) is shown in Fig. 3 as a function of particle energy in the detector active volume ($E_{ion}-\Delta E_{contact}$) for ^{4}He, ^{9}Be, and ^{32}S ions, together with the electronic stopping powers and nuclear stopping powers. For clarity purposes, a comparison of the same silicon detector response with the nuclear stopping powers on a finer scale is shown as insets. Ions of ^{4}He, ^{9}Be, and ^{32}S are chosen to represent three different cases of electronic stopping powers (dE/dx_{ele}). For ^{4}He ions in Fig. 3(a), the ion energies are in the region where dE/dx_{ele} increases with decreasing ion energy; for ^{32}S ions in Fig. 3(c), the ion energies are in the region where dE/dx_{ele} increases with increasing ion energy. For ^{9}Be ions in Fig. 3(b), the ion energies cover both sides of the stopping maximum, i.e., dE/dx_{ele} increases with increasing ion energy till reaching the Bragg maximum and then decreases with further increase in ion energy. While no correlation can be observed between the nonlinear response of silicon and the increase/decrease in dE/dx_{ele}, a clear mirror image between the silicon response and dE/dx_{nucl} is evident, as shown by the insets.

Correction of origin (2) requires understanding and modeling of energy partitioning. Under ion irradiation, energy is lost, at different energy deposition density (stopping power dE/dx) to both electrons (dE/dx_{ele}) and atoms (dE/dx_{nucl}), in materials over a depth, up to a few tens of micrometer. In the beginning of the energy loss process at high energies, the ion loses its energy mainly through electronic energy deposition, and travels along a nearly straight path. As the ion

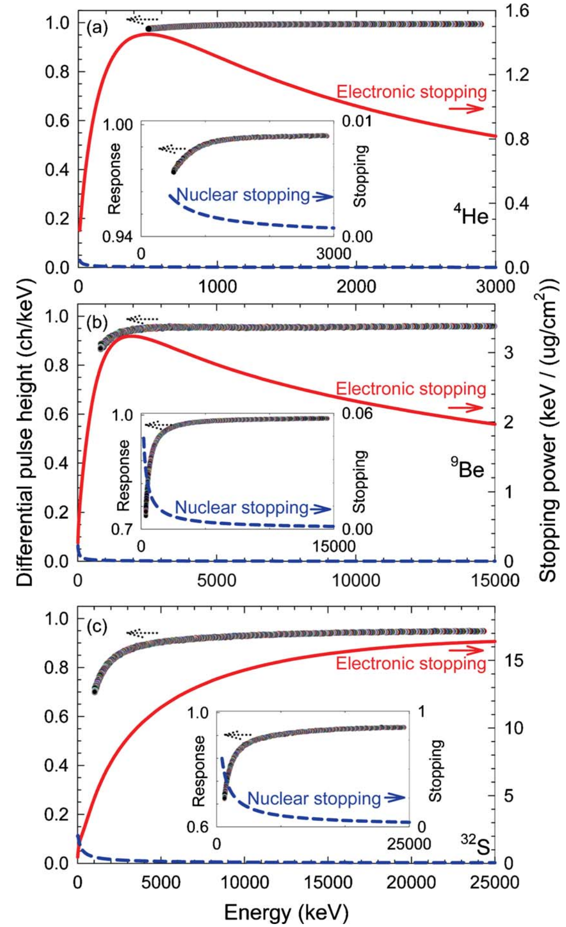

FIG. 3. (Color online) Detector differential pulse height in arbitrary unities and stopping of (a) ^{4}He, (b) ^{9}Be, and (c) ^{32}S ions as a function of particle energy with origin (1) corrected ($E_{ion}-\Delta E_{contact}$). The insets are the comparison of the differential response behavior with the nuclear stopping as a function of $E_{ion}-\Delta E_{contact}$.

energy decreases, the probability of collisions with atomic nuclei increases and the nuclear stopping finally dominates the slowing-down process. The energy transferred from an ion to an atomic nucleus in a single collision is often many times greater than the energy threshold to displaced the atom from its site, resulting in atomic defects and, in some cases, more energetic secondary recoils that can travel within the material, lose energy to electrons and displace other atoms, creating a cascade of atomic collision events. Energy transfer to the target electrons creates e-h pairs (inner shell holes and energetic primary electrons) and inelastic electron-electron scattering.[17,18] Kinetic-energy transfer to atoms that does not contribute to e-h pair production can result in permanent displacements of atoms from their lattice sites, thereby forming atomic-scale defects. Since the number of e-h pairs produced by a charged particle is related to the electronic energy deposition from both the primary ion and the silicon recoils within the detector active volume, the total ion energy is separated, using the Stopping and Range of Ions in Matter (SRIM) 2008 simulations,[19] into electronic energy deposition (E_{ele}) to create e-h pairs and nonelectronic energy deposition (E_{non}) resulting in lattice vibrations, crystal damage, and

other energy deposition processes into the system (instead of creating e-h pairs). The energy loss that does not contribute to e-h pair production, origin (2), can be corrected by using SRIM 2008.01 full-cascade simulations[19] to model energy partitioning. For a given element at a given energy, the energy partitioning between E_{ele} and E_{non} in silicon can be calculated under the assumptions of a sample density of $2.321\ \mathrm{g\ cm^{-3}}$ and Si threshold displacement energy of 15 eV.[20–22]

The effect of origin (2) on nonlinear response of silicon to ion irradiation is shown in Fig. 2. The response for "Origin (2) corrected" (the upper curve) is the measured pulse height normalized to $E_{\mathrm{ele}}(=E_{\mathrm{ion}}-\Delta E_{\mathrm{contact}}-E_{\mathrm{non}})$, the energy producing e-h pairs in the detector active volume. Due to the extremely thin contact layer of the ion-implanted detectors used in this study, the impact of origin (1) is shown to be not as significant as origin (2). It is also evident that the correction for origin (2) is more critical at lower energies, less than a few hundreds of keV/amu, which is consistent with the mirror correlation between the silicon response and dE/dx_{nucl}, shown as the insets in Fig. 3.

It has been commonly accepted that a high rate of e-h recombination, origin (3), is expected in the dense plasma create along the path of heavy ions due to the high electronic stopping powers.[1,3,5] If e-h pairs recombine at a higher rate in the dense plasma due to higher energy deposition rate, a lower collected electronic signal is expected for high electronic stopping powers (higher dE/dx_{ele}), which is generally accepted as the dominating contribution to the PHD. It is worth noting that the electronic stopping power is a function of ion energy, and it varies along the ion path as the ion slows down, as shown by the solid lines in Fig. 3. The same number of e-h pairs due to the same amount energy deposition can be produced within a smaller volume when the electronic stopping power is higher. In Fig. 3, the silicon response is the measured value of e-h pairs created along the ion path in the detector active volume normalized to $E_{\mathrm{ion}}-\Delta E_{\mathrm{contact}}$. The stopping power values used in Fig. 3 are the SRIM calculated values for the ions just reaching the detector active volume after passing through the contact layer, which is not directly related to the silicon response to the whole slowing-down process.

To validate the third origin to the nonlinearity and PHD, collection of e-h pairs for a small energy deposition over a small ion range should be evaluated, where e-h pair production can be assumed to be uniformly produced over the small ion range, and the e-h pairs collected for the same amount of deposited energy but over different length scale can be compared. Since the electronic signals, in this study, are collected for multimillion ions with energies over a continuous range, as shown in Fig. 1, it is possible to determine the difference in electronic signals from a small energy difference, such as between E_{ele} and $E_{\mathrm{ele}}-\Delta E_{\mathrm{ele}}$, where E_{ele} varies from the energy close to the maximum ion energy produced from the accelerator and the energy that ions barely penetrate the contact layer, and ΔE_{ele} can be a few keV or just 1 keV. The difference in electronic signals between E_{ele} and $E_{\mathrm{ele}}-1$ keV is plotted as a function of dE/dx_{ele} at ion energy of $E_{\mathrm{ele}}-0.5$ keV. The corresponding results for ^{1}H, ^{4}He, ^{9}Be, ^{28}Si, and ^{32}S are shown in Fig. 4, a perfect horizontal trend

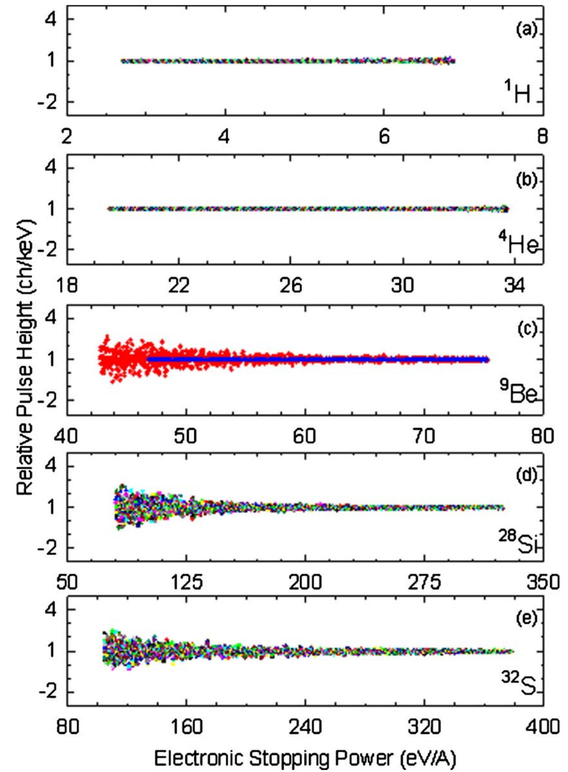

FIG. 4. (Color online) Small differences in electronic signals between E_{ele} and $E_{\mathrm{ele}}-1$ keV as a function of electronic stopping powers (dE/dx_{ele}) at energy of −0.5 keV under of (a) ^{1}H, (b) ^{4}He, (c) ^{9}Be, (d) ^{28}Si, and (e) ^{32}S ion bombardments.

versus the electronic stopping powers over a wide region from ∼2.5 to 380 eV/Å is observed. No indication of the high rate of e-h recombination is observed at higher electronic stopping powers, as for H^{+} and He^{+} irradiation where dE/dx_{ele} decreases with increasing ion energy, for Be^{+} where dE/dx_{ele} both increases and decreases with increasing ion energy, and for Si^{+} and S^{+} where dE/dx_{ele} increases with increasing ion energy. Especially for the case of Be ions, with increasing energy and dE/dx_{ele} from ∼43 to ∼76 eV/Å, the data points (diamonds) becomes more clustered together. With further increase in ion energy, dE/dx_{ele} decreases to ∼47 eV/A, where the relative pulse height (dots) overlays in the middle of the diamond points.

It is known that the silicon band gap (1.12 eV) is much larger than the thermal noise at room temperature (∼1/40 eV), providing excellent signal to noise ratios, and eliminating the need for cooling except in ultralow noise applications. The main source of noise in the silicon crystal itself is the energy spread due to the electronic energy loss straggling and the statistical fluctuations in the number of charge carriers produced. Both contributions of the energy straggling and charge carrier fluctuation decrease with increase in ion energy, which can be observed under all irradiations in Fig. 4. For the H^{+}, He^{+}, Si^{+}, and S^{+} irradiations, the relative pulse height at different energies is shown by various points with different shapes and colors; for the Be^{+} irradiations the result is shown as diamond points for energies lower than the Bragg peak, and in dots for the energies above the peak. The largest energy spread is clearly shown

by the scatter of the data points at lower energies, such as at ~42 eV/Å for Be^+, ~80 eV/Å for Si^+, and close to 100 eV/Å for S^+. The continuous reduction in energy spread is observed with the increasing energy. The influence from the energy loss straggling and the statistical fluctuations in the number of charge carriers is negligible for light ions, such as H^+ and He^+, and for higher energy heavy ions with energies close to the Bragg maximum and above, such as Be^+ (>75 eV/Å), Si^+ (>325 eV/Å), and S^+ (>380 eV/Å).

The results shown in Fig. 4 clearly demonstrate that the high rate of e-h recombination in the dense plasma for heavy ions due to high electronic stopping power is a false assumption. Significant trapping of the e-h pairs with increasing atomic defects created by heavy ions through nuclear collisions is the predominate contribution to the nonlinear response, as shown by the upper curves in Fig. 2. Trapping of the e-h pairs is also noticeable at higher energies for He, Be, and S, which leads to PHD as shown by the deviation of the response from the unity value determined by H ions, as indicated by the dashed lines in Fig. 2.

The results and the methodology in the current work have long-reaching implications for radiation science that involves both semiconductors and scintillators. The energy cascade in a radiation detector precedes in much the same manner for semiconductors and scintillators through the generation of information carriers (electron-hole pairs). In semiconductor materials, the electrons and holes are swept apart by an electric field, and the resulting induced charge is measured on metal electrodes at the surface of the material. The current study could have important implications for nonsilicon, advanced semiconductor detectors used under extreme conditions. In inorganic scintillators, the electrons and holes recombine at activation sites, which relax via photon emission. The primary differences between semiconductors and scintillators arise in electron-hole transport and subsequent charge measurement or photon emission processes. The mechanisms of light yield nonproportionality, a critical scintillation property, are currently under intensive investigations. The experimental approach demonstrated in this study for a Si detector can be used to investigate the nonlinearity, electrons and holes recombination (directly related to the number of photons emitted per unit of ionizing energy loss) as a function of electronic stopping powers over a continuous energy region. Such studies will provide fundamental understanding on nonlinear radiation response to ionization/excitation and transport properties in advanced semiconducting and scintillating materials, and the knowledge will provide a pathway for predicting relationships between material properties and performance. It will avoid Edisonian approaches for advanced detector material discovery, and lead to the ability to design complex or structured materials with improved performance that would not likely been discovered otherwise.

IV. CONCLUSION

In current investigation, the response of a silicon detector (the most used detector type) to single-ion excitation is studied for different ions over a continuous energy region to evaluate the origins of pulse height defect and nonlinearity. For the same electronic energy deposition, but with different dE/dx_{ele}, recombination and trapping behaviors of the same number of e-h pairs produced within different volume along the ion path are investigated. Through the material response to such unique excitation conditions, the e-h pair recombination rate and trapping behaviors are determined. The results indicate that, beside the contribution of energy loss in the surface contact layer, high rate recombination is not observed for heavy ions in the region where higher density plasma is expected. On the other hand, significant trapping is explicitly observed with increasing atomic defects created by heavy ions through nuclear energy deposition that leads to both nonlinear response at low energies and pulse height defect at high energies.

ACKNOWLEDGMENTS

The authors are grateful to the staff at the Tandem Laboratory, Uppsala University, Sweden for accelerator operations and experimental assistance. This work was supported by the Materials Sciences & Engineering Division, Office of Basic Energy Sciences, U.S. Department of Energy.

---

*Author to whom correspondence should be addressed: Oak Ridge National Laboratory, 4500S (B148), MS 6138, Oak Ridge, Tennessee 37831-6138; zhangy1@ornl.gov

[1] *Radiation Detection and Measurement*, 3rd ed., edited by G. F. Knoll (Wiley, New York, 2000), Chap. 11.
[2] R. A. Langley, Nucl. Instrum. Methods **113**, 109 (1973).
[3] E. C. Finch and A. L. Rodgers, Nucl. Instrum. Methods **113**, 29 (1973).
[4] J. B. Mitchell, S. Agami, and J. A. Davies, Radiat. Eff. **28**, 133 (1976).
[5] E. C. Finch, M. Asghar, and M. Forte, Nucl. Instrum. Methods **163**, 467 (1979).
[6] E. C. Finch, F. Gonnenwein, P. Geltenbort, A. Oed, and E. Weissenberger, Nucl. Instrum. Methods **228**, 402 (1985).
[7] M. Ogihara, J. Nagashima, W. Galster, and T. Mikumo, Nucl. Instrum. Methods Phys. Res. A **251**, 313 (1986).
[8] W. N. Lennard, H. Geissel, K. B. Winterbon, D. Phillips, T. K. Alexander, and J. S. Forster, Nucl. Instrum. Methods Phys. Res. A **248**, 454 (1986).
[9] E. C. Finch, Nucl. Instrum. Methods Phys. Res. A **257**, 381 (1987).
[10] W. N. Lennard and K. B. Winterbon, Nucl. Instrum. Methods Phys. Res. B **24-25**, 1035 (1987).
[11] Y. Zhang, H. J. Whitlow, and T. Winzell, Nucl. Instrum. Methods **161-163**, 297 (2000).
[12] T. D. M. Weijers, J. A. Davies, R. G. Elliman, T. R. Ophel, and H. Timmers, Nucl. Instrum. Methods Phys. Res. B **190**, 387 (2002).

[13] Y. Zhang and W. J. Weber, Nucl. Instrum. Methods Phys. Res. B **267**, 1705 (2009).
[14] Y. Zhang, H. J. Whitlow, T. Winzell, I. F. Bubb, T. Sajavaara, K. Arstila, and J. Keinonen, Nucl. Instrum. Methods Phys. Res. B **149**, 477 (1999).
[15] Y. Zhang, Nucl. Instrum. Methods Phys. Res. B **196**, 1 (2002).
[16] Y. Zhang, B. D. Milbrath, W. J. Weber, M. Elfman, and H. J. Whitlow, Appl. Phys. Lett. **91**, 094105 (2007).
[17] Y. Zhang, I.-T. Bae, and W. J. Weber, Nucl. Instrum. Methods Phys. Res. B **266**, 2828 (2008).
[18] S. E. Derenzo, M. J. Weber, E. Bourret-Courchesne, and M. K. Klintenberg, Nucl. Instrum. Methods Phys. Res. B **505**, 111 (2003).
[19] J. F. Ziegler, SRIM-SRIM 2006, http://www.srim.org
[20] J. C. Barbour, D. Dimos, T. R. Guilinger, and M. J. Kelly, Nanotechnology **3**, 202 (1992).
[21] M. V. Ramana Murty and H. A. Atwater, Phys. Rev. B **45**, 1507 (1992).
[22] M. J. Caturla, T. D. de la Rubia, and G. H. Gilmer, J. Appl. Phys. **77**, 3121 (1995).